AIP | Applied Physics Letters

Gd@Au15: A magic magnetic gold cluster for cancer therapy and bioimaging

Brahm Deo Yadav and Vijay Kumar

Citation: Appl. Phys. Lett. **97**, 133701 (2010); doi: 10.1063/1.3491269
View online: http://dx.doi.org/10.1063/1.3491269
View Table of Contents: http://apl.aip.org/resource/1/APPLAB/v97/i13
Published by the American Institute of Physics.

$Gd@Au_{15}$: A magic magnetic gold cluster for cancer therapy and bioimaging

Brahm Deo Yadav[1,2] and Vijay Kumar[1,a)]
[1]*Dr. Vijay Kumar Foundation, 1969 Sector 4, Gurgaon, 122001 Haryana, India*
[2]*Centre for Modelling and Simulations, University of Pune, Ganeshkhind, Pune 411007, India*

(Received 9 July 2010; accepted 29 August 2010; published online 27 September 2010)

We report from *ab initio* calculations a magic magnetic cage cluster of gold, $Gd@Au_{15}$, obtained by doping of a Gd atom in gold clusters. It has a highest occupied molecular orbital-lowest unoccupied molecular orbital gap of 1.31 eV within the generalized gradient approximation that makes it a potential candidate for cancer therapy with an additional attractive feature that its large magnetic moment of 7 μ_B could be beneficial for magnetic resonance imaging. © *2010 American Institute of Physics*. [doi:10.1063/1.3491269]

Colloidal gold has been used from ancient times to produce different colors in stained glasses and potteries and it has been believed to cure many deceases. In recent years, gold nanoparticles have been discovered[1] to be very effective in cancer therapy while surprisingly gold clusters become very good catalyst[2] even though bulk gold is the most noble metal. These findings have fueled research on gold clusters and nanoparticles to understand their properties and to prepare doped nanogold.[3] Experiments[4] on Gd doped Au nanoparticles show magnetism that could lead to their application in magnetic resonance imaging (MRI). We have carried out *ab initio* calculations on Gd doped Au clusters and found a magic cluster $Gd@Au_{15}$ which has the attractive features of a large highest occupied molecular orbital-lowest unoccupied molecular orbital (HOMO-LUMO) gap and a large magnetic moment that could make it useful for both phototherapies of cancer cells as well as bioimaging.

Earlier efforts[5] to dope Au clusters with transition metal (TM) atoms such as Ti, V, and Cr in Au_6 and Fe, Co, and Ni in Au_{16} have shown atomiclike magnetic moments on the TM atom. However, doping[6] of a Cr, Mo, or W atom in Au_{12} and other metal atoms[7,8] in different sized gold clusters to prepare stable effectively 18 valence electron doped gold clusters quenches the magnetic moment of the metal atom completely. Therefore, the magnetic behavior of a TM atom in Au clusters is dependent on the environment. On the other hand, *f* orbitals in rare earths are highly localized and could lead to high magnetic moments that are less sensitive to local environment. We therefore doped gold clusters with a Gd atom that has the highest magnetic moment.

Gold clusters with up to 15 atoms have planar structures[9] and thereafter three-dimensional (3D) structures become favorable. With Gd doping, an interesting question is the effect on their atomic structures. We find that some small $GdAu_n$ clusters continue to favor planar structures, but beyond n =9, 3D structures are the lowest in energy. All clusters have high magnetic moments, and therefore, doping of Gd is better to produce magnetic nanogold than TMs. Here we present our finding of $Gd@Au_{15}$ with a cage structure of Au_{15} that has the most attractive features for biomedical applications.

The calculations have been performed by using projector augmented wave pseudopotential plane wave method[10] with spin-polarized generalized gradient approximation[11] (GGA) for the exchange-correlation energy. The cluster was placed in a large cubic cell and the Brillouin zone integrations were done using only the Γ point. The electronic energy and ionic forces were converged within 0.0001 eV and 0.005 eV/Å without imposing any symmetry constraint and for the calculation of the vibrational spectrum, further convergence was achieved within 10^{-5} eV and 0.001 eV/Å, respectively. For Au we considered 11 valence electrons while for Gd, the valence configuration is taken to be $5s^25p^64f^75d^16s^2$ with 18 electrons. The cutoff energy for the plane wave expansion is taken to be 400 eV.

Figures 1(a) and 1(b) (different view) show the lowest energy optimized structure of $Gd@Au_{15}$ in which a Gd atom is encapsulated in the cage of Au_{15}. Gd atom is bigger than a gold atom and 15 Au atoms are optimal around it. Gd interacts with all the 15 Au atoms with small variation in the Au–Gd bond lengths (2.94–3.18 Å). However, there is a larger variation in Au–Au bond lengths that lie in the range of 2.72–3.37 Å. This result suggests a preference to optimize Au–Gd bonding in $Gd@Au_{15}$. It is because of the fact that the binding energy of an Au–Gd dimer is 3.54 eV as compared to 2.34 eV for an Au–Au dimer. The Au_2 (Au–Gd)

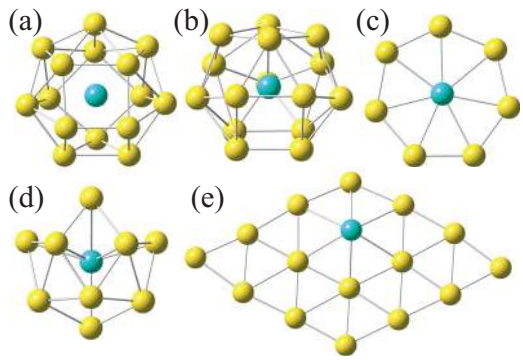

FIG. 1. (Color online) (a) Atomic structure of $Gd@Au_{15}$ with Gd atom inside Au_{15} cage. (b) is another view of the same structure. Gold and Gd atoms are shown in golden (light grey in print) and blue (dark grey in print) colors. (c) The lowest energy structure (nearly planar) of $GdAu_7$. (d) FK isomer of $Gd@Au_{15}$ and (e) a planar isomer of $GdAu_{15}$ with a capped hexagon.

a)Author to whom correspondence should be addressed. Tel./FAX: +91-124-4079369. Electronic mail: kumar@vkf.in.

bond length is 2.52 (2.67) Å. The Au–Gd dimer also has a magnetic moment of 7 μ_B. Therefore, Au–Gd bond is much stronger as compared to Au–Au bond. A similar behavior was obtained[12] for metal encapsulated Si clusters in which the interaction between a TM atom and Si is much stronger as compared to Si–Si and this leads to cage structures of Si clusters. In our case the structure of the Au_{15} cage in $Gd@Au_{15}$ cluster is very different from the lowest energy structure of neutral Au_{15} which is planar as well as a low lying 3D isomer which lies only 0.13 eV higher in energy than the planar structure.[13] Therefore, Gd doping affects the structure of Au clusters very significantly.

The atomic structure of $Gd@Au_{15}$ was obtained (1) by optimizing a Frank–Kasper (FK) isomer[12] of $TM@Si_{15}$ and (2) by adding two atoms to the structure of $Au_{13}Gd$ obtained in the growth behavior of Gd doped Au clusters. The FK isomer [Fig. 1(d)] is stable at lower convergence of force but finally goes to the same structure [Fig. 1(a)] when accuracy of convergence is increased. The bicapped structure of $GdAu_{13}$ also converges to the lowest energy isomer [Fig. 1(a)] that has a central buckled ring of seven Au atoms and a Gd atom at the center [see Fig. 1(b)]. There are two slightly distorted squares, one on each side of this ring and rotated with respect to each other by about 45°. Interestingly the lowest energy atomic structure of Au_7Gd is nearly planar with a ring of Au_7 and Gd at the center [Fig. 1(c)]. Gd atom being larger than a gold atom, favors seven Au atoms to form a ring around it. It is another magic cluster with a large HOMO-LUMO gap. Buckling of this ring provides better interaction with the two squarelike units of Au atoms in $Gd@Au_{15}$. The gain in energy by doping a Gd atom in Au_{15} cage is about 9.5 eV. We also optimized the Au_{15} cage of $Gd@Au_{15}$ to find if it is favorable for Au_{15}. The optimized cage structure is a FK polyhedron and it lies 0.5 eV higher in energy compared with the planar structure.[13] Further, doping of a Gd atom in planar structures [Fig. 1(e)] with a capped heptagon as well as a structure based on Au heptagon) leads to isomers that are about 3 eV higher in energy than the isomer in Fig. 1(a). Vibrational spectrum of the lowest energy isomer[13] has all positive frequencies suggesting the stability of this cluster.

The binding energy of $Gd@Au_{15}$, defined with respect to free atoms, is 2.641 eV/atom. It is higher than 2.222 eV/atom and 2.196 eV/atom for Au_{15} planar and a FK cage isomer of Au_{16}, respectively. Therefore, $Gd@Au_{15}$ is energetically much more stable than pure Au clusters of similar sizes. Also it has a high magnetic moment of 7 μ_B and a large HOMO-LUMO gap of 1.31 eV within GGA that make it useful for multifunctional biomedical applications. The large magnetic moment in $Gd@Au_{15}$ is nearly localized on Gd atom with only a small polarization around Au atoms as shown in Fig. 2. The localized nature of the magnetic moments and the fact that Gd atom is encapsulated in Au cage, make it very interesting for applications at the nanoscale.

The electronic structure of $Gd@Au_{15}$ as well as Au_{15} cage in which the positions of the Au atoms have been kept the same as in $Gd@Au_{15}$ and only the Gd atom has been removed is shown in Fig. 3. In Fig. 3(a) Gd 5*s* and 5*p* levels are not shown. The electronic structure of Au_{15} cage shows [Fig. 3(b)] a large energy gap after 18 electron counting, excluding the 5*d* electrons of Au atoms. Accordingly, the stability of $Gd@Au_{15}$ cluster can be understood by considering a spherical jellium model in which fifteen 6*s* electrons

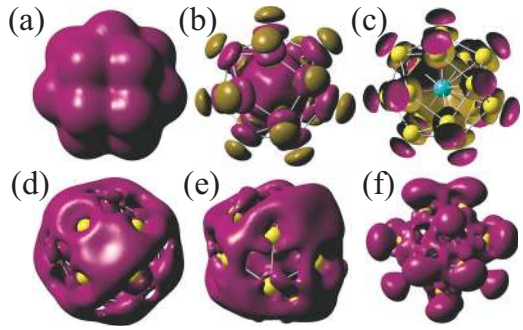

FIG. 2. (Color online) (a) Isosurface (value 0.148 e/Å^3) of the total electronic charge density, [(b) and (c)] spin-polarization isosurfaces (0.000 59 per Å^3), respectively, for up- and down-spins of $Gd@Au_{15}$. In (b) down-spin polarization [mustard color (light grey in print)] is seen around Au atoms but in (c) there is absence of down-spin polarization [violet color (dark grey in print)] around the Gd atom. [(d) and (e)] (different views) show the isosurface of the excess (0.0015 e/Å^3) and (f) the depletion (0.000 59 e/Å^3) of the electronic charge density obtained by subtracting the sum of the charge densities of Au_{15} cage and a Gd atom at the same positions as in $Gd@Au_{15}$ and the charge density of $Gd@Au_{15}$. Some charge is transferred from the top of Au atoms and around the Gd atom while an excess of charge is seen in between Au atoms as well as between Au_{15} cage and Gd atom [see the view in (f)].

of Au atoms occupy 1*s* and 1*p* states fully while the 1*d* states near the HOMO are only partially occupied leaving three holes. As Gd atom is trivalent, doping of a Gd atom leads to the stability of this cluster within 18 valence electron rule. The 4*f* electrons on Gd atom remain unpaired and contribute to the net magnetic moment of 7 μ_B on $Gd@Au_{15}$. The

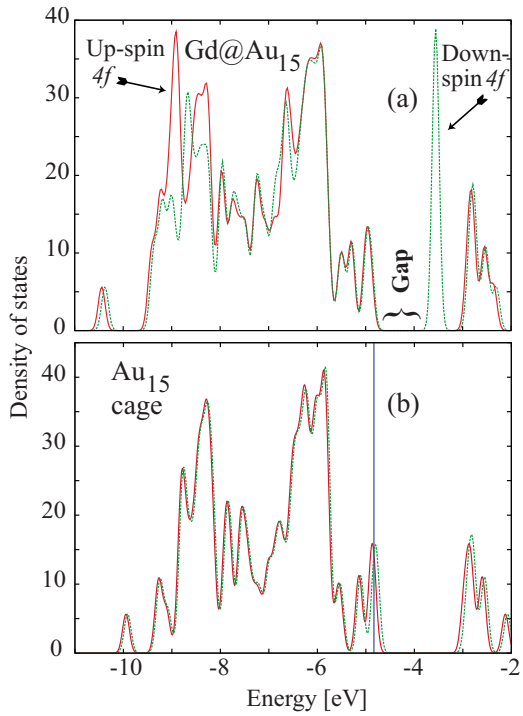

FIG. 3. (Color online) (a) Gaussian broadened (half width 0.05 eV) electronic levels of $Gd@Au_{15}$. The 4*f* levels of Gd are marked. The red (dark grey in print) and green (light grey in print) curves are for up and down spin states, respecitvely. Notice a large HOMO-LUMO gap. (b) The Gaussian broadened electronic levels of Au_{15} cage with the Au atoms placed at the same positions as in $Gd@Au_{15}$. There is a large gap after 18 valence electrons excluding the 5*d* electrons on Au atoms. The vertical line shows the HOMO. One can see some holes in the states just above the HOMO. Also there is redistribution of the Au 5*d* states after encapsulation of a Gd.

up-spin $4f$ levels of Gd lie in the energy range of the $5d$ levels of gold and hybridize significantly with the latter. In the spherical jellium model, the $1d$ orbitals of the Au_{15} cage hybridize with the $5d$ orbitals of Gd while the $6s$ electrons get transferred to the unoccupied $1d$ states of the Au_{15} cage as inferred from a state in the unoccupied region with predominantly s character of Gd atom.

In Fig. 2 we have shown the electronic charge density as well as the difference in the electronic charge densities of $Gd@Au_{15}$ and the sum of the charge densities of Au_{15} cage and an isolated Gd atom at the same positions as in the Gd encapsulated cage. From these results, we find a charge transfer from near the top of Au atoms and around the Gd atom to regions in between the gold atoms as well as between gold cage and the Gd atom—a reflection of some covalent bonding character in the cluster. These features of the bonding are seen in the electronic density of states. The up-spin $4f$ states lie in the energy range of -10 to around -8 eV while the unoccupied $4f$ down-spin states lie at around the energy of -3.5 eV within the HOMO-LUMO gap of the Au_{15} cage as it can be seen in Fig. 3(b). The electronic states near the HOMO arise from Au atoms and are of $1d$ character in the jellium model. One can see a shift in some states in this region to higher binding energy in going from Au_{15} cage to $Gd@Au_{15}$. Also the density of states corresponding to Au $5d$ levels gets affected after interaction with Gd showing significant Au $5d$–Gd $4f$ hybridization.

The HOMO-LUMO gap of $Gd@Au_{15}$ is underestimated within GGA and we expect the true value to lie in the red to infrared region and this makes $Gd@Au_{15}$ cluster interesting for cancer therapy. We also explored $Gd@Ag_{15}$ but the HOMO-LUMO gap is only 0.57 eV in GGA. Further other trivalent atoms such as La, Y, and Sc stabilize the cage structure of Au_{15} but these clusters are nonmagnetic and have large HOMO-LUMO gap of about 2 eV within GGA. The presence of the down-spin $4f$ states of Gd within the HOMO-LUMO gap is significant and it makes $Gd@Au_{15}$ particularly attractive. The large magnetic moment can have dual advantage of potential application for MRI also.

In summary we have obtained from *ab initio* calculations a magic magnetic cluster of gold, $Gd@Au_{15}$ with a large HOMO-LUMO gap of 1.31 eV that can be useful for phototherapy of cancer cells. Furthermore there are large magnetic moments localized on Gd atom and this makes $Gd@Au_{15}$ also attractive for bioimaging. The magnetic moments in Gd doped gold clusters are only weakly sensitive to the local environment as both Au_7Gd and $Gd@Au_{15}$ with very different structures, have 7 μ_B magnetic moments. Therefore doping of rare earths and particularly Gd is better as compared to TM atoms to form magnetic nanostructures of gold. We hope our work would stimulate experimental realization of $Gd@Au_{15}$ cluster and exploration of its biomedical applications.

We thankfully acknowledge partial financial support from Asian Office of Aerospace Research and Development (AOARD) for materials simulation (Grant No. FA4869-078-1-4063). We are grateful to the staff of the Centre for the Development of Advanced Computing (CDAC) for allowing the use of their computer resources as well as for their technical support. B.D.Y. thanks P. P. Shinde for many helpful discussions.

[1]X. Huang, P. K. Jain, I. H. El-Sayed, and M. A. El-Sayed, Nanomedicine **2**, 681 (2007).
[2]A. A. Herzing, C. J. Kiely, A. F. Carley, P. Landon, and G. J. Hutchings, Science **321**, 5894 (2008); See also Tiny Gold Clusters Are Top-notch Catalysts, http://www.sciencedaily.com /releases/2008/09/080905215954.htm.
[3]V. Kumar, Phys. Rev. B **79**, 085423 (2009); **80**, 039902(E) (2009).
[4]Y. T. Lim, M. Y. Cho, B. S. Choi, J. M. Lee, and B. H. Chung, Chem. Commun. (Cambridge) **2008**, 4930.
[5]X. Li, B. Kiran, L.-F. Cui, and L.-S. Wang, Phys. Rev. Lett. **95**, 253401 (2005); L.-M. Wang, J. Bai, A. Lechtken, W. Huang, D. Schooss, M. M. Kappes, X. C. Zeng, and L. S. Wang, Phys. Rev. B **79**, 033413 (2009).
[6]P. Pyykkö and N. Runeberg, Angew. Chem., Int. Ed. **41**, 2174 (2002); X. Li, B. Kiran, J. Li, H.-J. Zhai, and L.-S. Wang, *ibid.* **41**, 4786 (2002).
[7]Y. Gao, S. Bulusu, and X. C. Zeng, ChemPhysChem **7**, 2275 (2006).
[8]S. Neukermans, E. Janssens, H. Tanaka, R. E. Silverans, and P. Lievens, Phys. Rev. Lett. **90**, 033401 (2003).
[9]B. Yoon, P. Koskinen, B. Huber, O. Kostko, B. von Issendorff, H. Häkkinen, M. Moseler, and U. Landman, ChemPhysChem **8**, 157 (2007).
[10]G. Kresse and D. Joubert, Phys. Rev. B **59**, 1758 (1999); P. E. Blöchl, Phys. Rev. B **50**, 17953 (1994).
[11]J. P. Perdew, in *Electronic Structure of Solids '91*, edited by P. Ziesche and H. Eschrig (Akademie, Berlin, 1991).
[12]V. Kumar and Y. Kawazoe, Phys. Rev. Lett. **87**, 045503 (2001); V. Kumar, Comput. Mater. Sci. **36**, 1 (2006); V. Kumar, in *Nanosilicon*, edited by V. Kumar (Springer, Oxford, 2008).
[13]See supplementary material at http://dx.doi.org/10.1063/1.3491269 for Fig. S1 for the structures and Fig. S2 for the spectrum.